JOURNAL OF CATALYSIS 33, 414–419 (1974)

Synthetic Offretite

III. Physicochemical Aspects of Crystallization

E. L. WU, T. E. WHYTE, JR., M. K. RUBIN AND P. B. VENUTO

Process Research and Technical Service Division, Mobil Research and Development Corporation, Paulsboro, New Jersey 08066

Received December 6, 1973

The progress of crystallization of tetramethylammonium (TMA) offretite from an alumina–silica gel at 97°C has been monitored by sorptive, thermochemical, spectroscopic, and other physicochemical probes. Initial ordering of gel particles into large agglomerates and onset of crystallization occurred within the first 20 hr. During the critical interval of 20–44 hr, the gel was transformed into a crystalline phase, with incorporation of aluminum and TMA cations into the aluminosilicate lattice, and after this period showed all characteristics of crystalline offretite, including maximum sorption capacity and typical crystal morphology.

INTRODUCTION

In an earlier report (*1*) of crystallographic, morphologic and thermochemical properties of synthetic offretite, we related thermal removal of the bulky intracrystalline tetramethylammonium (TMA) cations to the appearance of significant cyclohexane sorption capacity. Decomposition of the organic cations was later shown to be associated with the appearance of protonic acidity (*2*). As in the case of ZK-4 (*3*) and the N-Q and N-R aluminosilicates (*4*), the nitrogenous cations in offretite are incorporated during synthesis, and thus may be expected to play an important role in directing the crystallization of the zeolite (*5*). Recent studies on the synthesis of Linde A and faujasite using phosphorescence and laser–Raman spectroscopy have been reported by McNicol *et al.* (*6*, *7*).

We now describe results of a study in which the progress of crystallization of TMA–offretite is monitored by sorptive, thermochemical, spectroscopic, and other physicochemical probes. These data provide insights into the timing of incorporation of aluminum and TMA cations into the zeolite framework, the development of sorption capacity, and other aspects of the offretite synthesis mechanism.

EXPERIMENTAL METHODS

Materials

Nalco 680 $NaAlO_2$ (43.8% Al_2O_3), Du Pont Ludox LS (30% SiO_2) and Baker reagent grade chemicals were used in the offretite synthesis. *n*-Hexane (Phillips 99% pure) and water (distilled) were employed as adsorbates.

Crystallization and Sampling Techniques

The offretite was synthesized from an alumina–silica gel in the presence of potassium, sodium, and tetramethylammonium hydroxides by the method of Jenkins (*8*). Crystallization was carried out at 97°C without stirring in a sealed polypropylene container. Representative aliquots (40 ml) were withdrawn periodically from the reaction mixture. The samples were quenched rapidly by filtering off the mother liquor and washing with distilled water to pH 10. All samples were dried in air at 105°C for at least 3 hr prior to analyses.

Analytical Procedures

X-Ray diffraction patterns were obtained using a Siemens powder diffractometer (Cu$K\alpha$ radiation) with strip chart and pulse height analyzer. Relative crystallinities were calculated by comparison to a known standard. Electron microscopic examinations were carried out using an RCA EMU-3 electron microscope. A Du Pont differential thermal analyzer, Model 900, was used for DTA analysis. All infrared spectra were recorded using pressed KBr pellets (0.5 mg samples) on a Perkin-Elmer 421 spectrophotometer. Sorption capacities of the samples (calcined 16 hr at 550°C) were determined using a semiautomatic adsorption apparatus (*9*).

Results

Elemental and Structural Analyses

Elemental analyses and relative X-ray crystallinities of samples periodically withdrawn from the reaction mixture are given in Table 1. A trace of crystalline material was identified at 19.5 hr and crystallization was apparently 85% complete at about 28 hr. The sample after 43.5 hr was identified as 100% crystalline offretite.

Electron photomicrographs of solid samples are shown in Figs. 1 and 2. A general ordering of gel particles into large agglomerates was observed during the initial 22.5-hr induction period (Fig. 1a and b). Typical offretite crystallites have appeared by 25.5 hr (Fig. 1c). Consistent with the X-ray finding, no irregular-shaped gel particles were found in the 43.5-hr sample (Fig. 1d).

Thermal Analyses

DTA patterns of solid samples are shown in Fig. 3. The development of the characteristic DTA profile reported for high purity TMA–offretite (*1*) is clearly shown. The initial fine structure at 4 hr evolves into a broad endotherm with minimum near 800°C after 25.5 hr. Weak endotherms near 370 and 430°C, and a relatively sharp endotherm near 550°C become clearly resolved in the 28-hr sample—consistent with an observed X-ray crystallinity of 85%. The first two endotherms are associated with the decomposition of the TMA cations. The subsequent dehydroxylation of the protonic acid sites so generated is reflected in the sharp endotherm near 550°C (*1*, *2*).

Sorption Measurements and Rate of Crystal Growth

Typical sorption curves for water and *n*-hexane are illustrated in Fig. 4. The sorption capacity of the solid material for both sorbates was relatively low during the first

TABLE 1

Elemental Analyses and Relative X-Ray Crystallinities of Solid Samples

Reaction time (hr):	0	9	19.5	22.5	28	43.5	91	357.5[c]
X-Ray cryst (%)[a]:	Amorph.	Amorph.	Tr	45	85	100	—	125
Elemental analysis[b] (g/100 g)								
N	0.01	0.031	—	0.21	—	—	—	1.16
K	2.04	13.3	—	13.1	—	8.03	8.59	8.70
Na	0.71	2.17	—	2.77	—	0.75	1.09	1.27
Al_2O_3	3.8	16.3	—	14.9	—	15.3	15.0	15.1
SiO_2	93.3	67.5	—	68.1	—	74.4	73.8	74.0
SiO_2/Al_2O_3	41.7	7.03	—	7.76	—	8.25	8.35	8.31

[a] Peak height of diffraction line at $2\theta = 23.5°$, relative to a standard sample. Since crystallizing offretites may have variations in the number, type, and lattice location of cations, a limitation is placed upon quantitative assessment of X-ray line intensities. Nevertheless, the X-ray data are in essential agreement with the sorption data.

[b] Sample moisture levels were not controlled prior to nitrogen analysis; all other analyses are on ignited basis.

[c] BET (N_2) surface area = 350 m^2/g.

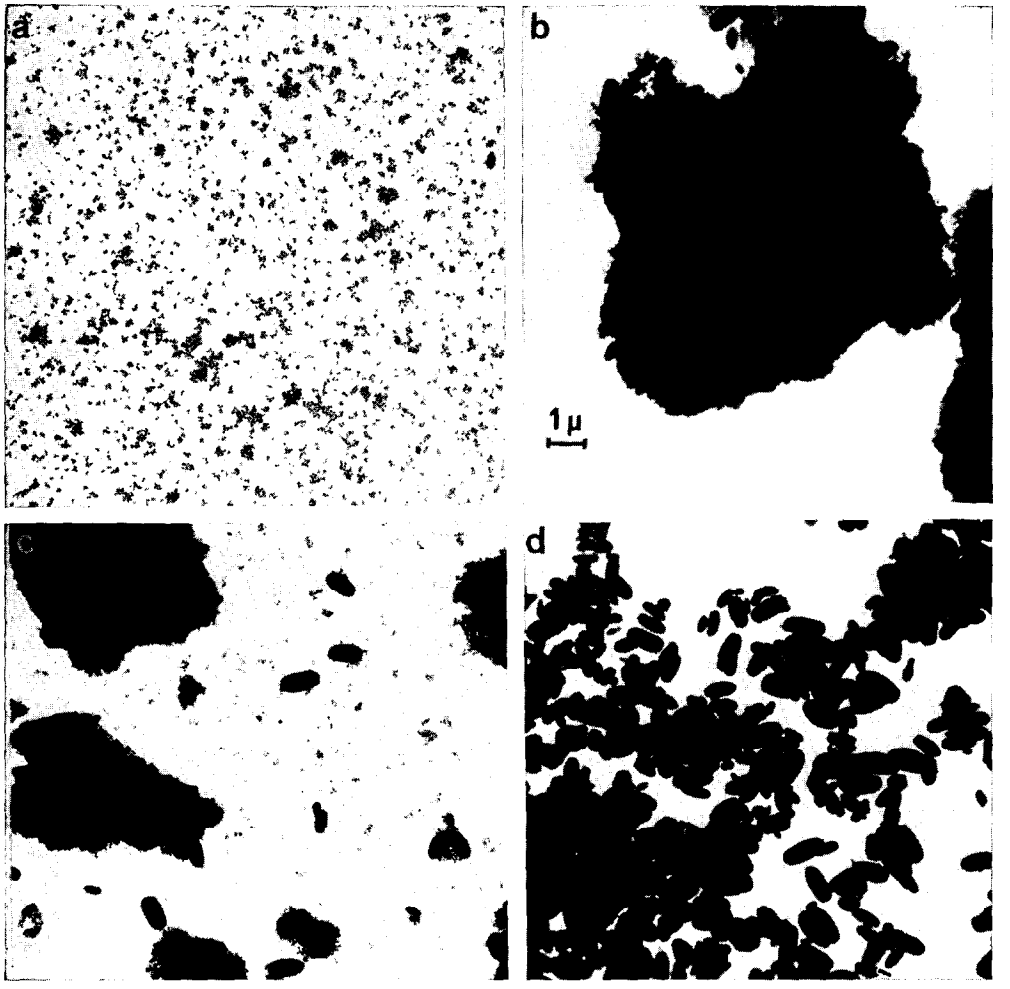

FIG. 1. Electron photomicrographs of TMA–offretite crystallization. 4500×. (a) 19.5 hr; (b) 22.5 hr; (c) 25.5 hr; (d) 43.5 hr.

22.5 hr, but then increased rapidly to a maximum near 43.5 hr.

Infrared (ir) Analysis

Infrared spectroscopic examination of the same series of samples showed distinct changes in important vibrational frequencies as crystallization proceeded. Trends occurring in the position of vibrational bands assigned to the aluminosilicate framework are shown in Fig. 5, together with the major ir frequencies of the reactants—Ludox and $NaAlO_2$. Samples taken after 43.5 hr showed all ir bands characteristic of crystalline offretite.

The two bands in the 600–800 cm^{-1} region were separately resolved into several bands after about 19.5 hr, and their overall intensities greatly increased during the 20–43.5-hr crystallization period but remained unchanged thereafter (Fig. 6).

Changes in the ir bands arising from the tetramethylammonium (TMA) cation with crystallization time are shown in Figs. 5 and 6 also. Most interesting is the CH_3-deformation (δ_{CH_3}) band near 1484 cm^{-1}; after 22.5 hr, this was resolved into two distinct bands, and its intensity increased markedly during the early crystallization period, reaching a maximum at about 74 hr (Fig. 6). In addition a C–N stretching band near 950 cm^{-1} became apparent after 43.5 hr.

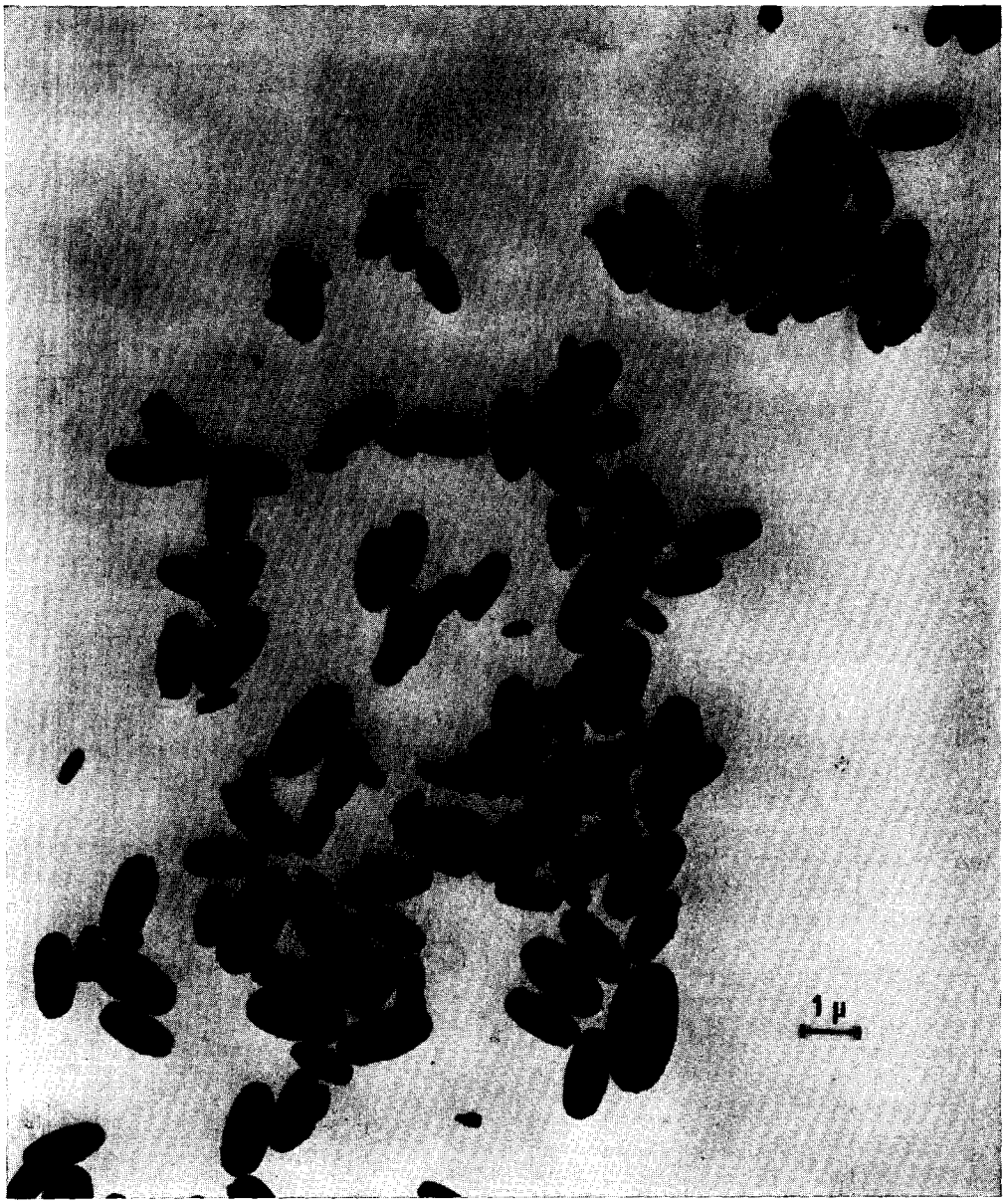

FIG. 2. Electron photomicrographs of TMA-offretite crystallization. 9000×. 50 hr.

DISCUSSION

Emergence of Crystallinity and Incorporation of Aluminum

During the "induction period" of the first 20 hr at 97°C, the frequency of the ν_{Si-O} band (appearing initially at 1110 cm^{-1}) shifted to 1035 cm^{-1}, but little evidence of crystalline offretite was observed. Since the frequency of this band decreases as SiO_2/Al_2O_3 ratio decreases (*10*, *11*), aluminum incorporation into the amorphous gel phase (or silica solubilization from the gel) is indicated. This is consistent with aluminum analysis data (Table 1). Further ir changes—reflecting slight upward adjustments in the SiO_2/Al_2O_3 ratio—occurred at about 20 hr, the onset of crystal nucleation.

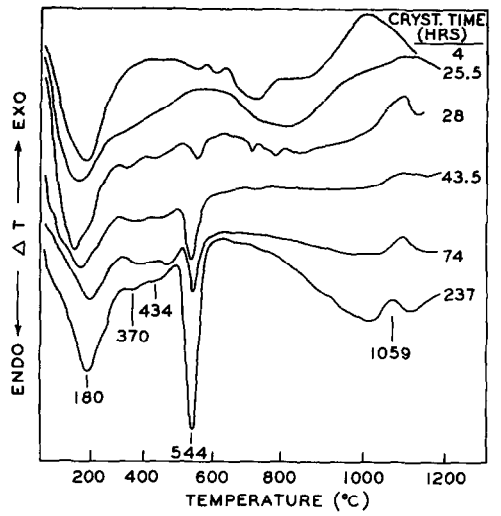

FIG. 3. Differential thermal analysis in TMA–offretite synthesis. Temp scan, 30°C/min; atm–N_2, 150 ml/min; sample size, 50 mg; reference, Al_2O_3; ΔT(mV/in.), 0.008 (0.02 for 43.5 and 74 hr); thermocouples, Pt–Pt, 13% Rh.

During the critical interval of 20–44 hr, the gel was transformed into a crystalline phase. Significant changes in crystal morphology and in the overall cation content and relative proportions of potassium and sodium were also observed. Samples removed after 43.5 hr residence showed all characteristic properties of crystalline TMA–offretite:

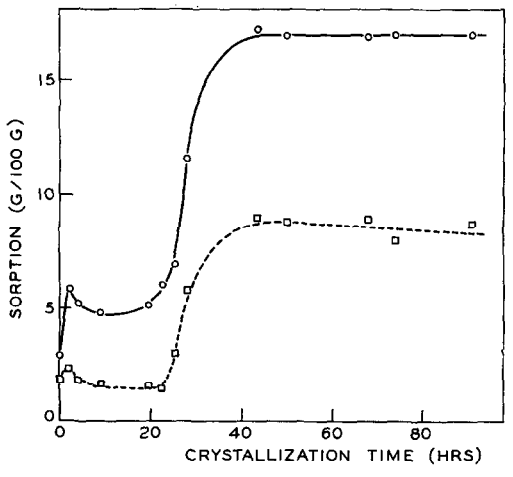

FIG. 4. Sorption measurements in TMA–offretite synthesis. (○) H_2O; P/P_0 = 0.50 at 25°C; (□) $n-C_6$; P/P_0 = 0.13 at 25°C. Samples calcined in air for 16 hr at 482°C.

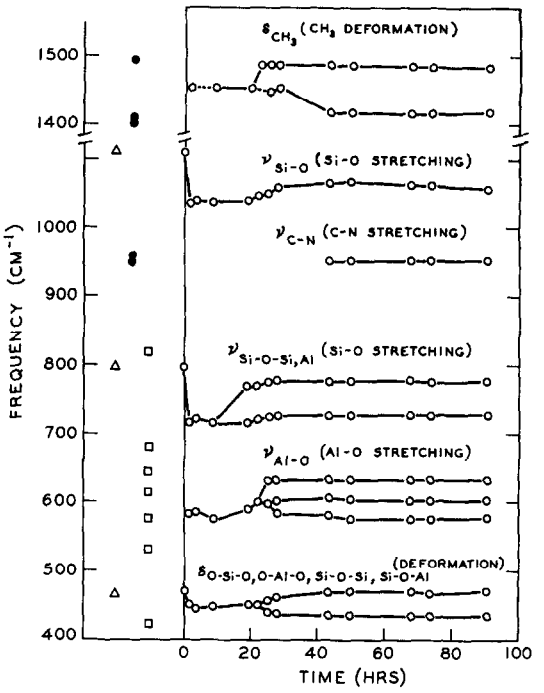

FIG. 5. Infrared absorption frequency versus crystallization time. Reactants: Ludox (△); $NaAlO_2$ (□); TMA chloride (●); products: offretite (○).

100% crystallinity (Table 1), characteristic DTA profile (Fig. 3) and ir spectrum (Fig. 5), maximum sorption capacity (Fig. 4) and typical irregular-shape morphology (Fig. 2). It follows that the crystallization period of

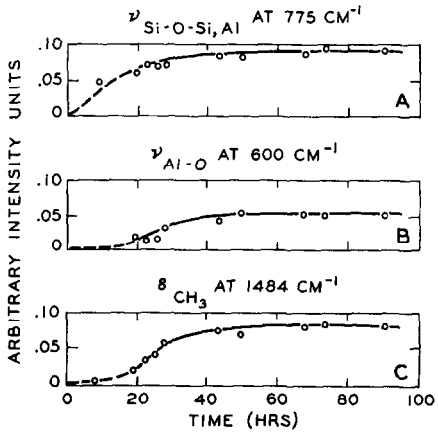

FIG. 6. Infrared band intensity versus crystallization time. Intensity = (peak height of band)/(peak height of ν_{Si-O}).

TMA–offretite need not be extended beyond 2 days. Assuming that maximum sorption capacity corresponds to 100% conversion of amorphous to crystalline aluminosilicate, application of the method of Ciric (*12*) to the data in Fig. 4 predicts 100% conversion of amorphous mixture to crystalline offretite in about 30 hr.

A number of the infrared bands, including peaks at 775 and 600 cm^{-1}, were observed in the offretite sample (Figs. 5 and 6). Stubican and Roy (*13*) have assigned a band near 775 cm^{-1} in aluminosilicates to stretchings involving coupled vibrators Si–O–Al or Si–O–Si. The appearance and increase in intensity of such a band in the offretite system (Fig. 6A) may relate to incorporation of aluminum into a crystalline lattice environment. Bands in the vicinity of 600 cm^{-1}, present in the starting aluminate but not in the silica, may be associated with Al–O bond stretches. Recently, Flanigen, Szymanski and Khatami (*11*) have associated bands at about 775 and 600 cm^{-1} in the infrared spectra of zeolites to extratetrahedral vibrations due to coupling of tetrahedra which may or may not contain aluminum. Such bands are characteristic for each zeolite, and their appearance in the present case correlates directly with the concentration of zeolite offretite in the product.

Incorporation of TMA Cations

Paralleling the increase in crystallinity (or zeolitic aluminum) was an increase in intensity of infrared bands due to TMA cations (Figs. 5 and 6C), suggesting the incorporation of the organic cations into the zeolite. This conclusion is supported by the nitrogen analyses (Table 1). TMA cations appear to play an important role in the crystal growth mechanism of the relatively open offretite structure. The initial growth phase may involve formation of gmelinite cages around TMA templates. Cations in such an environment could not be removed by simple ion exchange. The nitrogenous cations may also play a role in effecting formation of the main channel system. Similar thinking has been advanced by Aiello and Barrer (*5*) and Aiello *et al.* (*14*) in studies of TMA–zeolite systems, including an offretite-like composition.

Acknowledgments

We thank Dr. J. Cattanach for performing the thermochemical analyses, Mr. G. R. Landolt and Mr. J. H. Wuertz for their excellent technical assistance, and Mr. S. Sawruk for the electron photomicrographs. We thank Professor W. M. Meier of Eidgenössische Techniche Hochschule of Zürich, Switzerland, for encouragement at the initiation of this study.

References

1. Whyte, T. E., Jr., Wu, E. L., Kerr, G. T., and Venuto, P. B., *J. Catal.* **20,** 88 (1971).
2. Wu, E. L., Whyte, T. E., Jr., and Venuto, P. B., *J. Catal.* **20,** 384 (1971).
3. Kerr, G. T., *Inorg. Chem.* **5,** 1537 (1966).
4. Barrer, R. M., and Denny, P. J., *J. Chem. Soc. (London)*, 971 (1961).
5. Aiello, R., and Barrer, R. M., *J. Chem. Soc. A*, 1470 (1970).
6. McNicol, B. D., Pott, G. T., and Loos, K. R., *J. Phys. Chem.* **76,** 3388 (1972).
7. McNicol, B. D., Pott, G. T., Loos, K. R., and Mulder, N., *Advan. Chem. Ser.* **121,** 152 (1973).
8. Jenkins, E. E., *U.S. Pat.* 3,578,398 (May 11, 1971).
9. Landolt, G. R., *Anal. Chem.* **43,** 613 (1971).
10. Wright, A. C., Rupert, J. P., and Granquist, W. T., *Amer. Mineral.* **53,** 1293 (1968).
11. Flanigen, E. M., Szymanski, H. A., and Khatami, H., *Advan. Chem. Ser.* **101,** 201 (1971).
12. Ciric, J., *J. Colloid Interface Sci.* **28,** 315 (1968).
13. Stubican, V., and Roy, R., *Z. Kristallogr.* **115,** 200 (1961).
14. Aiello, R., Barrer, R. M., Davies, J. A., and Kerr, I. S., *Trans. Faraday Soc.* **66,** 1610 (1970).